Progress In Electromagnetics Research Letters, Vol. 38, 137–150, 2013

SYNTHESIS OF A SINGLE SIDE ACCESS RING RESONATOR FOR HIGHER ORDER BANDPASS FILTERS

Norfishah A. Wahab*, Mohd K. M. Salleh, Sameh K. M. Khanfar, Zuhani I. Khan, and Zaiki Awang

Microwave Technology Centre, Faculty of Electrical Engineering Universiti Teknologi MARA (UiTM), Shah Alam, Selangor 40150, Malaysia

Abstract—A single-side-access ring resonator topology is presented. It employs a single quarter-wavelength coupled-line that couples to a one-wavelength ring to exhibit a single-mode resonance with transmission zeros. A global synthesis is presented, in order to control the transmission zeros in its response. As the transmission zeros of the ring resonator maintains their positions when multiple identical rings are used, the global synthesis can further be used for the design of higher order filters with multiple rings. Furthermore, since only one coupled-line is used in the resonator topology, only one section of line is present in the ring, other than the coupled-line. Hence, there will be no second section of the ring that needs to be adjusted to obtain the symmetrical response during its realization, as compared to other types of ring topologies. To show the advantage of the synthesis, it is applied in the design of higher order ring-based bandpass filters, which also involve extra quarter-wavelength coupled-lines to create additional poles. Five bandpass ring filters up to 5th-order were realized using microstrip technology, and measured to validate the proposed concept. Measurement results showing good agreement with those from the simulation are also presented throughout the paper.

1. INTRODUCTION

Bandpass filter topology with high selectivity, miniaturized size, low loss and ease of reproducibility is highly solicited for present microwave communication systems. Amongst various topologies available, ring-based topology is well known for its dual mode capability, compact size

Received 28 December 2012, Accepted 12 March 2013, Scheduled 14 March 2013

* Corresponding author: Norfishah Ab Wahab (fishahahu@yahoo.com.my).

and sharp rejection skirts [1–10]. Early work done by Wolff had shown that, two degenerate orthogonal modes, TM_{10} and TM_{01} coexist in a symmetrical ring resonator [1]. By having perturbation elements such as stubs, patches or notches on the ring, internal coupling is created to split the two modes.

In order to generate the dual resonance, most of the dual-mode ring resonator topologies require adjustment of their coupling points and perturbation elements [2–8]. The work reported by [9, 10] made use of quarter-wavelength coupled lines in the ring topology that led to a global synthesis, based on the control parameters: Z_r, Z_{oe} and Z_{oo}, which are the impedance of the ring, and the even- and odd-mode impedance of the coupled lines, respectively. A problem of such topology is that, the two lines of impedance Z_r in the ring need to be of identical physical length, which limits the freedom to control the symmetrical form of its response. The problem is even more significant when multiple rings were used in higher order filters. Furthermore, the synthesis of the ring resonator with two coupled-lines is limited to a single resonator and is not generalized at present for higher order filters with multiple rings. For instance, the transmission zeros of a higher order filter with multiple rings will not follow the initial position of the transmission zeros of a single ring.

In this paper, the proposed ring topology employs a single quarter-wavelength coupled-line, which is coupled to a one-wavelength ring. The response still contains the transmission zeros but only a single resonance is obtained instead of dual resonance. A global synthesis of the single-side-access ring resonator is presented in order to control the transmission zeros of its response. It will be shown that the synthesis can also be used for the design of higher order bandpass filters. In fact, the main advantage of such topology is that, only one section of line with impedance Z_r is present in the resonator, eliminating the second length adjustment problem when trying to obtain the symmetrical bandpass response if two coupled-lines are used. Such advantage is even more significant when multiple rings are used for higher order filters. Moreover, the transmission zeros of the ring resonator maintain their positions when multiple identical rings are used to obtain higher order bandpass response. This means, the global synthesis of the resonator presented in this paper can further be used in fixing the transmission zeros and the bandwidth of higher order filters with multiple rings.

In the next section, the single mode ring topology is presented, complete with the development of its synthesis that helps to fix transmission zeros. The synthesis is then used to design higher order filters in which extra coupled-lines are introduced in the configuration to create additional poles. A total of four higher order bandpass filters are proposed, having 2nd, 3rd, 4th and 5th order. Finally, to verify the proposed idea, five bandpass ring resonators up to 5th order are realized using full-wave electromagnetic simulator, fabricated using microstrip technology, and measured.

2. TOPOLOGY AND SYNTHESIS OF THE SINGLE SIDE ACCESS RING RESONATOR

Figure 1 shows the single-side-access ring topology with a quarter-wavelength coupled-line. A three-quarter-wavelength line of impedance Z_r is connected at its extremities to a quarter-wavelength coupled-line with even- and odd-mode impedances of Z_{oe} and Z_{oo} respectively, to form a one-wavelength ring at a given center frequency f_o. Figure 2 shows an example of the resonator's ideal response with $f_o = 1\,\text{GHz}$, $Z_r = 90\,\Omega$, $Z_{oe} = 70\,\Omega$ and $Z_{oo} = 35\,\Omega$.

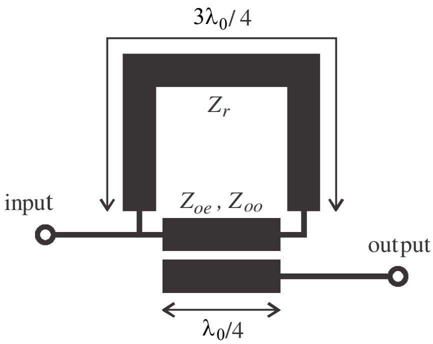

Figure 1. Single-side-access ring resonator basic cell topology.

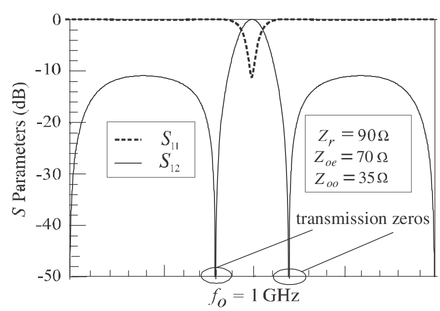

Figure 2. Ideal response of the single-side-access ring resonator.

2.1. Equivalent Circuit of the Ring Resonator

Starting from the definitions and parameters of a 3-port coupled-lines given by [11–13], a simplified circuit diagram of the ring resonator can be constructed and shown in Figure 3. The definition of the elements in the diagram such as the transformer T, the unit element Y_{ue} and the coupling capacitor Y_c are given in Appendix. These elements, and hence, the response of the resonator, are functions of the impedances Z_r, Z_{oe} and Z_{oo}. Running a circuit simulation of the diagram in Figure 3 with the same value of impedances given earlier, where $f_o = 1\,\text{GHz}$, $Z_r = 90\,\Omega$, $Z_{oe} = 70\,\Omega$ and $Z_{oo} = 35\,\Omega$, will give the same results as shown in Figure 2.

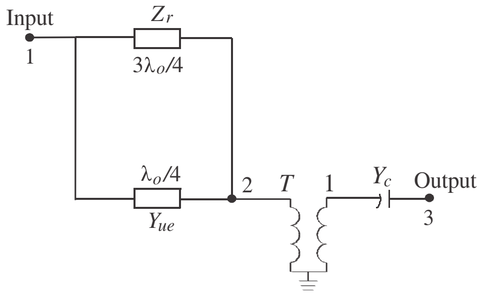

Figure 3. Equivalent circuit diagram of the single-side-access ring resonator.

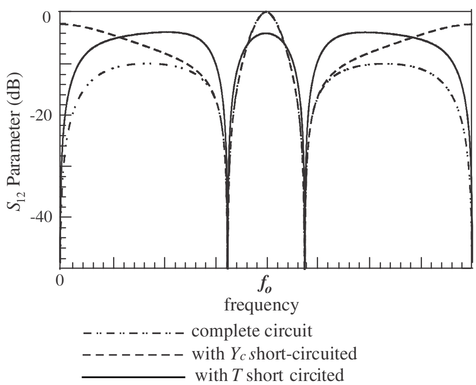

Figure 4. Simulated frequency response of the single-side-access ring resonator for three different cases: response of the complete circuit, response of the circuit when the transformer is short-circuited, and response when the coupling capacitor is short-circuited.

Figure 4 illustrates the response of the circuit for three different cases: response of the complete circuit, response of the circuit when the transformer is short-circuited, and response when the coupling capacitor is short-circuited, for $f_o = 1\,\text{GHz}$, $Z_r = 90\,\Omega$, $Z_{oe} = 70\,\Omega$ and $Z_{oo} = 35\,\Omega$. As the positions of the transmission zeroes remain unchanged for in all the three cases, it can be concluded that the transformer and the coupling capacitor have no control on the position of the transmission zeros. In fact, the coupling capacitor Y_c only controls the resonator's out-of-band response while the transformer of ratio T, which is independent of frequency, serves as a multiplier to the overall magnitude of the response. Indeed, the position of transmission zeros are controlled by the central closed loop which can be further simplified to form a quadripole, represented by a Y-matrix, Y_{LT}, as illustrated in Figure 5.

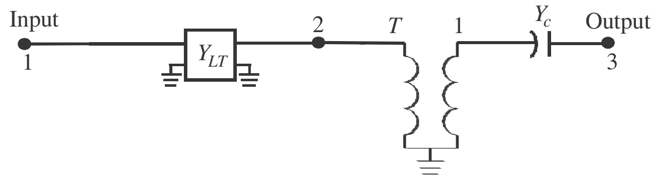

Figure 5. Simplified diagram of the single-side-access ring resonator.

2.2. Synthesis Equations and Transmission Zeros Control

The admittance matrix of the closed loop, Y_{LT} in Figure 3 is defined as follows:

$$Y_{LT} = \begin{bmatrix} Y_{LT11} & Y_{LT12} \\ Y_{LT12} & Y_{LT11} \end{bmatrix} \tag{1}$$

where,

$$Y_{LT11} = \frac{\left(4\cos\theta^2 - 3 + 4Y_{ue}Z_r\cos\theta^2 - Y_{ue}Z_r\right)\cos\theta}{jZ_r\sin\theta\left(4\cos\theta^2 - 1\right)} \tag{2}$$

$$Y_{LT12} = \frac{1 + 4CY_{ue}Z_r\cos\theta^3 - CY_{ue}Z_r\cos\theta}{\left(4\cos\theta^2 - 1\right)jZ_r\sin\theta} \tag{3}$$

$$C = \frac{\left(\tan\theta^2 + 1\right)}{\sqrt{1 + \tan\theta^2}} \tag{4}$$

From here, the transmission zero locations can be determined by equating the Y_{LT12} to zero, resulting to;

$$1 + 4CY_{ue}Z_r\cos\theta^3 - CY_{ue}Z_r\cos\theta = 0 \tag{5}$$

Thus, the electrical length of the transmission zero at the lower side can be deduced to be as follows;

$$\theta_{tz} = \arccos\left(\sqrt{\frac{1 - Y_{ue}Z_r}{1 + Y_{ue}Z_r}}\right) \tag{6}$$

Likewise, the electrical length of the transmission zero can also be written as follows;

$$\theta_{tz} = \frac{\pi f_{tz}}{2f_o} \tag{7}$$

Therefore, using (6) and (7), and for a given transmission zero frequency f_{tz}, the admittance unit element, Y_{ue} can also be written in terms of Z_r as follows:

$$Y_{ue} = \frac{1}{\left(-1 + 4\cos\left(\frac{1\pi f_{tz}}{2f_o}\right)^2\right)Z_r} \tag{8}$$

Since the response of this resonator is symmetrical, the position of the upper side transmission zero can be determined from the lower side of transmission zero and the center frequency.

Finally, Y_{oo} can be expressed in terms of Y_{ue} and Y_{oe}, as;

$$Y_{oo} = \frac{Y_{ue}Y_{oe}}{2Y_{oe} - Y_{ue}} \tag{9}$$

Equations (8) and (9) can now be used to determine the value of Z_{oo} for a desired transmission zero frequency, f_{tz}, while the other two parameters, Z_{oe} and Z_r, can be chosen arbitrarily.

Figures 6 and 7 illustrate the applications of these equations. In Figure 6, three bandwidths are chosen by fixing different values of f_{tz}, while fixing the center frequency arbitrarily at f_o. Figure 7 illustrates the effect of varying Z_r or Z_{oe} while fixing the position of transmission

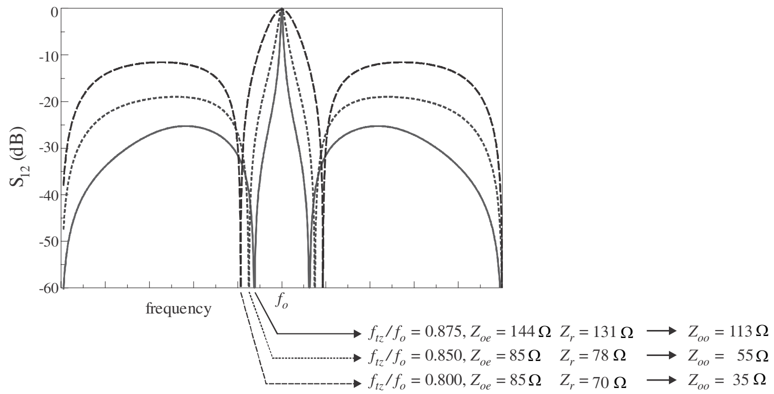

Figure 6. Application of the synthesis for three different sets of possible bandwidth, where the values of Z_{oo} are computed by Equations (8) and (9), for three different cases of f_{tz}.

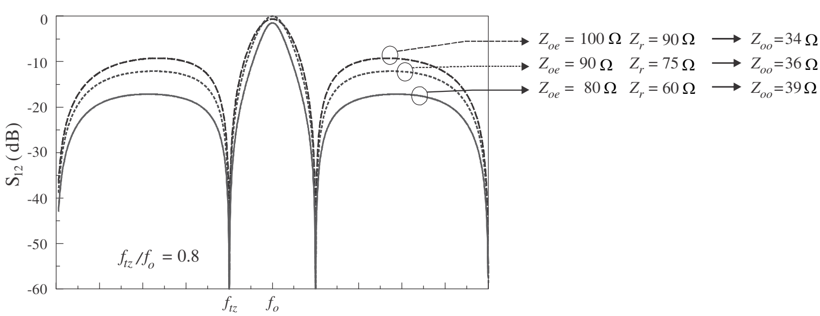

Figure 7. Application of the synthesis with variation of Z_r and Z_{oe}while f_{tz} is fixed at $0.8f_o$.

zeros, f_{tz}, to $0.8f_o$; in which the in-band and out-of-band response can be modified to the desired magnitude.

The basic ring resonator and its synthesis are further explored for higher order filter applications. For the investigation purposes, three higher order filter designs are discussed to investigate the behaviour of the resonators. As depicted in Figure 8, the first higher-order topology involves a series connection of the ring with a quarter-wavelength coupled line section to result in a 2nd order response. In the next topology, we employs two identical rings connected at their coupled-lines to produce a 3rd order filter. The third higher-order topology involves two identical basic rings with additional quarter-wavelength coupled-line to generate a 4th order response.

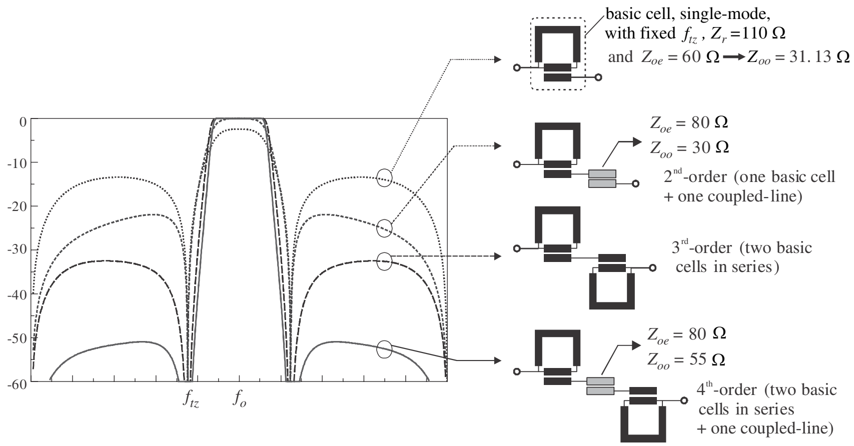

Figure 8. Examples of ideal resonance characteristics and topologies of the proposed higher-order bandpass filters.

The global synthesis of the base cell is applied to higher order filters to fix the position of the transmission zeros. The impedances Z_r and Z_{oe} are arbitrarily chosen to be equal to $110\,\Omega$ and $60\,\Omega$ respectively, which are typically in the range of realizable microstrip line impedance with a substrate thickness of 1.6 mm and ε_r of around 4, while Z_{oo} is given by Equation (9) to be equal to $31.13\,\Omega$. The even- and odd-mode impedances of the additional coupled-line in the 2nd and 4th order filters are $80\,\Omega$ and $30\,\Omega$, and $80\,\Omega$ and $55\,\Omega$, respectively. As illustrated in Figure 8, the transmission zeros' positions remain unchanged for all the three cases of higher order filter.

This observation has shown that the global synthesis of the basic ring can still be used to fix the transmission zeros for higher order filter design with multiple identical rings. As compared to the other types of basic ring resonator that make use of two coupled-line sections with synthesis, the proposed ring topology is simpler to design as it contains only one coupled-line section, while its synthesis can be used to maintain the position of the transmission zeros if two or more identical rings are to be used for higher order response. Hence, a designer can now obtain the value of Z_{oo} using the synthesis, for a desired position of transmission zeros, f_{tz} while Z_r and Z_{oe} can be chosen arbitrarily, depending on the desired in-band and out-of-band response magnitude.

3. APPLICATION OF THE SINGLE SIDE ACCESS RING RESONATOR FOR HIGHER ORDER FILTERS

3.1. Second Order Bandpass Filter Design — Single Ring with a Coupled Line

The basic ring is now combined with a quarter wavelength coupled-line at its output. The additional coupled-line results in a half-wavelength resonator formation and generates an extra pole in the passband response of the resonator. The 2nd-order filter is realized for a chosen center frequency of 2 GHz using FR-4 substrate ($\varepsilon_r = 4.1$, $h = 1.6$ mm and $\tan\delta = 2 \times 10^{-2}$). The overall layout with dimensions and electrical responses of the second order bandpass filter are depicted in Figures 9 and 10, respectively. Two transmission zeros are found at 1.78 GHz and 2.80 GHz with relative bandwidth of around 20% at 2.15 dB insertion loss.

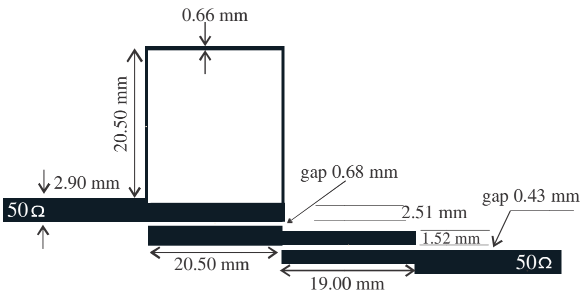

Figure 9. Layout of the 2nd order microstrip ring bandpass filter with a quarter wavelength coupled-line.

3.2. 3rd Order Bandpass Filter Design — Two Cascaded Rings

This design comprises two identical basic rings in series, which forms a half-wavelength resonator at the middle of the structure. A third

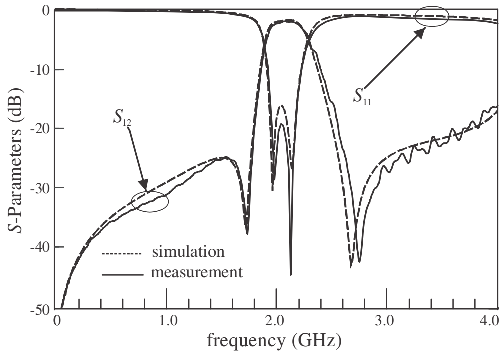

(a)

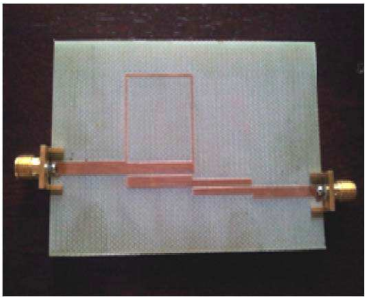

(b)

Figure 10. (a) Simulated and measured results of the 2nd order bandpass filter. (b) Photograph of the fabricated 2nd order microstrip ring bandpass filter.

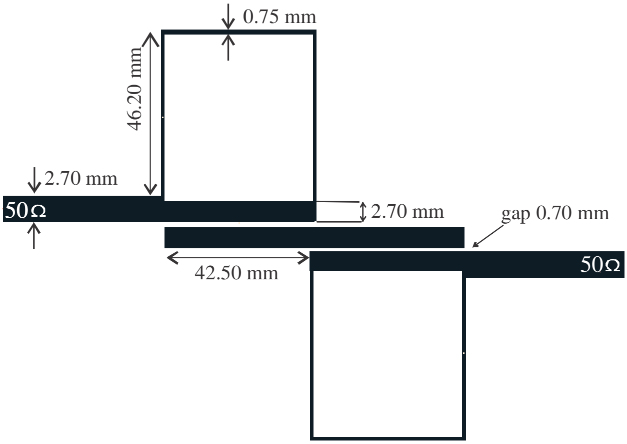

Figure 11. Layout of the 3rd order microstrip series-cascaded-rings bandpass filter.

pole is hence created leading to an overall 3rd-order bandpass filter. Designed at 1 GHz center frequency using FR-4 substrate ($\varepsilon_r = 4.1$, $h = 1.6$ mm and $\tan\delta = 0.02$), the overall layout and electrical responses of the filter are depicted in Figures 11 and 12, respectively. The relative bandwidth is found to be around 20% and the in-band insertion loss is 2.849 dB with a decent out-of-band rejection level of 30 dB up to 1.60 GHz.

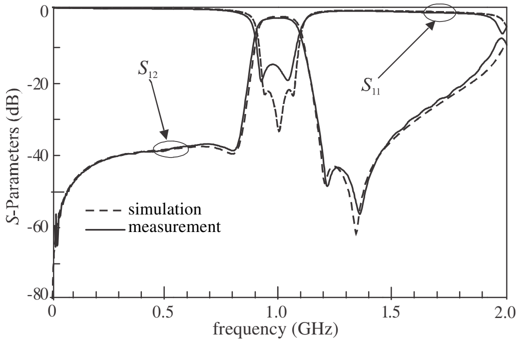

(a)

(b)

Figure 12. (a) Simulated and measured results of the 3rd order bandpass filter. (b) Photograph of the fabricated 3rd order series-cascaded-rings bandpass filter.

3.3. 4th-order Bandpass Filter Design — Two Cascaded Rings with A Coupled-line

An example of implementation of the 4th order bandpass resonator using microstrip technology is performed on Taconic substrate, for a chosen center frequency of 2 GHz. The characteristics of the substrate are given by: $\varepsilon_r = 4.5$, $h = 1.63$ mm and $\tan\delta = 3.5 \times 10^{-3}$. The design comprises of two identical rings in series, separated by an additional quarter-wavelength coupled-line in where two extra half-wavelength resonators are created to produce two additional poles. As a result, this topology generates four poles in the passband with two transmission zeros.

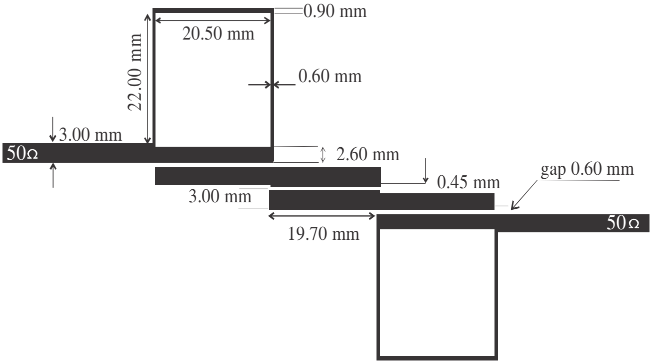

Figure 13. Layout of the microstrip 4th order series-cascaded-rings bandpass filter with a quarter wavelength coupled-line.

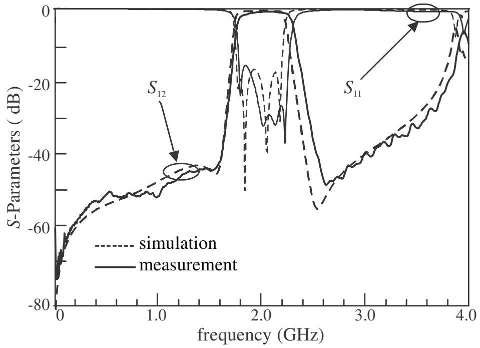

(a)

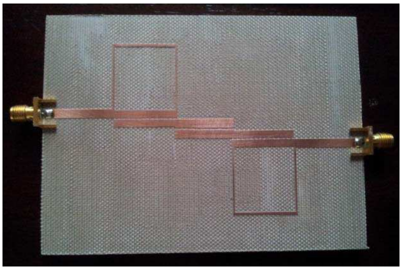

(b)

Figure 14. (a) Simulated and measured results of the 4th order bandpass filter. (b) Photograph of the fabricated 4th order bandpass filter.

The overall layout and electrical response of the bandpass filter are shown in Figures 13 and 14, respectively. The bandpass filter with two transmission zeros is observed having lower stopband at 1.54 GHz and upper stopband at 2.62 GHz. With 27% relative bandwidth, the in-band insertion loss is found to be 0.90 dB at 2.01 GHz centre frequency. The out-of-band rejection level of beyond 40 dB is found above up to 3 GHz.

3.4. 5th-order Bandpass Filter Design — Two Cascaded Rings with Two Coupled-lines

The cascaded rings concept is further explored. In this section, two identical basic cells are cascaded in series with additional two non-identical coupled-lines. Indeed, this arrangement produces three half-wavelength resonators, hence exhibits three additional poles. The 5th-order filter is realized on Taconic substrate at 2 GHz center frequency. The microstrip layout of the proposed filter is shown in Figure 15. As can be seen from this layout, the symmetrical aspect of the topology has been slightly disturbed to obtain extra freedom in order to attain a desired passband response.

As a result, an insertion loss of 1.24 dB is achieved as shown in Figure 16, with a good out-of-band rejection level of 30 dB up to 3 GHz. The transmission zeros are found at 1.55 GHz and 2.67 GHz with 26.55% relative bandwidth.

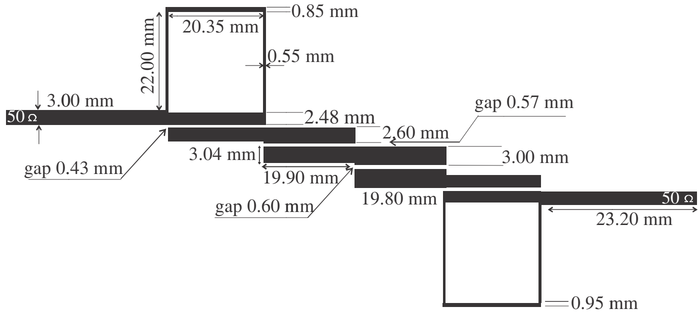

Figure 15. Layout of the 5th order series-cascaded-rings microstrip bandpass filter with two quarter wavelength coupled-lines.

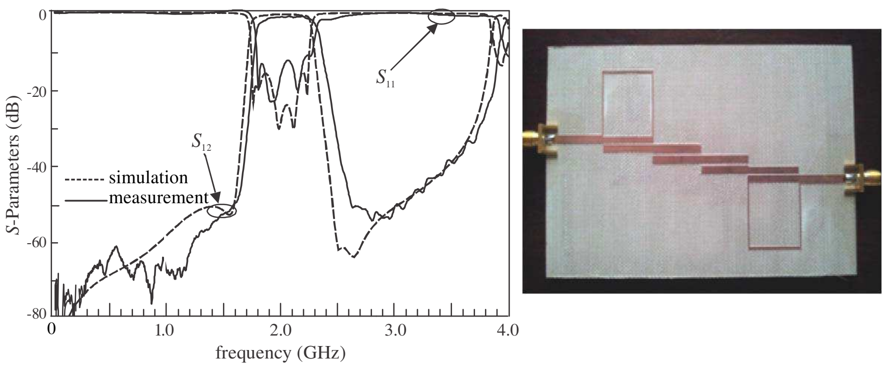

(a) (b)

Figure 16. (a) Simulated and measured results of 5th order bandpass resonator. (b) Photograph of the fabricated 5th order bandpass filter.

4. CONCLUSION

A synthesis of pseudo-elliptic single-side-access ring resonator was developed to control the position of its transmission zeros by varying its parameters, which were the line impedance of its elements. With a single coupled-line in the topology, realization of the resonator is simple, and the advantage can be extended to higher order filter design that involves cascade of multiple rings. Furthermore, its transmission zeros remain at the same position when two identical rings are put in series, even with further combination with other quarter-wavelength coupled-lines, which make its synthesis still valid for the higher order bandpass filter design. As compared to other types of basic ring resonator that make use of two coupled-line sections, the proposed ring topology is easier to design as it contains only one coupled-line section, thus no adjustment of second quarter-wavelength section needs to be done. In the meanwhile, its synthesis can be used to fix the transmission zeros for higher order filters. The ring was thereby proposed to be the base cell of four bandpass filters of different orders in microstrip technology as proofs of feasibility of the concept. The experimental data were found to be in good agreement with the theory and simulation results.

APPENDIX A.

Three-port coupled-line parameters [11–13]:

$$A_{ue} = \phi \begin{bmatrix} 1 & S/Y_{ue} \\ Y_{ue}S & 1 \end{bmatrix} \tag{A1}$$

$$Y_{ue} = Y_{11} - \frac{Y_{12}^2}{Y_{11}} \tag{A2}$$

$$\phi = \frac{1}{\sqrt{(1-s^2)}} \tag{A3}$$

$$s = j\tan\theta \tag{A4}$$

$$\theta = \frac{\pi f}{2f_o} \tag{A5}$$

$$Y_c = SY_{11} \tag{A6}$$

$$T = \frac{Y_{11}}{Y_{12}} \tag{A7}$$

$$Y_{11} = \frac{(Y_{oo} + Y_{oe})}{2} \tag{A8}$$

$$Y_{12} = \frac{(Y_{oo} - Y_{oe})}{2} \tag{A9}$$

$$Y_{oe} = \frac{1}{Z_{oe}} \tag{A10}$$

$$Y_{oo} = \frac{1}{Z_{oo}} \tag{A11}$$

REFERENCES

1. Wolff, I., "Microstrip bandpass filter using degenerate modes of a microstrip ring resonator," *Electronics Letters*, Vol. 8, No. 12, 302–303, Jun. 1972.
2. Luo, S. and L. Zhu, "A dual-mode dual-band bandpass filter using a single slot ring resonator," *Progress In Electromagnetics Research Letters*, Vol. 23, 173–180, 2011.

3. Chiou, Y. C. and P. S. Yang, "Transmission zero design graph for dual-mode dual-band filter with periodic stepped-impedance ring resonator," *Progress In Electromagnetics Research*, Vol. 108, 23–36, 2010.
4. Keshvari, M. and M. Tayarani, "A novel miniaturised bandpass filter based on complimentary split ring resonators (CSRRs) and open-loop resonators," *Progress In Electromagnetics Research Letters*, Vol. 23, 165–172, 2011.
5. Zhou, L., S. Liu, H. Zhang, X. Kong, and Y. Guo, "Compact dual-band bandpass filter using improved split ring resonators based on stepped impedance resontor," *Progress In Electromagnetics Research Letters*, Vol. 23, 57–63, 2011.
6. Liu, Y., X. Tang, Z. Zhang, and X. Huang, "Novel nested split-ring-resonator (SRR) for compact filter application," *Progress In Electromagnetics Research*, Vol. 136, 765–773, 2013.
7. Zhang, L., Z. Y. Yu, and S. G. Mo, "Novel planar multimode bandpass filters with radial-line stubs," *Progress In Electromagnetics Research*, Vol. 101, 33–42, 2010.
8. Prabhu, S. and J. S. Mandeep, "Microstrip bandpass filter at S band using capacitive coupled resonator," *Progress In Electromagnetics Research*, Vol. 76, 223–228, 2007.
9. Mohd Salleh, M. K., G. Prigent, O. Pigaglio, and R. Crampagne, "Quarter-wavelength side-coupled ring resonator for bandpass filters," *IEEE Transactions on Microwave Theory and Techniques*, Vol. 56, 156–162, Jan. 2008.
10. Ma, Z., H. Sasaki, C. Chun-Ping, T. Anada, and Y. Kobayashi, "Design of a wideband bandpass filter using microstrip parallel-coupled dual-mode ring resonator," *2010 Asia-Pacific Microwave Conference Proceedings (APMC)*, 21–24, 2010.
11. Ozaki, H. and J. Ishii, "Synthesis of a class of strip-line filters," *IRE Trans. on Circuit Theory*, Vol. 5, No. 2, 104–109, Jun. 1568.
12. Sato, R. and E. G. Cristal, "Simplified analysis of coupled transmission-line networks and their application (short paper)," *IEEE Transactions on Microwave Theory and Techniques*, Vol. 18, 122–131, 1970.
13. Nemoto, Y., K. Kobayashi, and R. Sato, "Graph transformations of nonuniform coupled transmission line networks and their application," *IEEE Transactions on Microwave Theory and Techniques*, Vol. 33, No. 11, 1257–1263, Nov. 1985.